

Property modeling integrating CPT's and UHRS datasets to define glacial geomorphology and related geo-engineering hazards.

Introduction

Offshore wind farm development is a critical component in the transition towards decarbonized energy production. Exploring shallow coastal bathymetry areas with both geophysical and geotechnical datasets is essential for detailed characterization of local geological settings. The Ten Noorden van de Waddeneilanden Wind Farm Zone (TNW), located in the Wadden sea (Quaternary sediments), is well suited for offshore foundation development given its proximity with the operating Gemini windfarm. An integrated study has been conducted on the characterization of geohazards and their probability of occurrence to support foundations drilling and cable backfilling operations (Bellwald et al. 2023). Particular attention has been given to 3D UHR Seismic interpretation and selection of Cone Penetration Tests (CPT's) logs to map specific soil properties within a newly created geomodel for later development steps. Regarding the location of TNW, this paper aims to provide insights into glacial geomorphology and its implications, focussing on geo-engineering hazard assessment prior to offshore wind farm site development. Emphasis is placed on precise characterisation of spatial variability within tunnel valleys and channels infills, highlighting changes in soil properties through modeling.

Geological settings

TNW is located offshore Netherlands, in the Dutch sector of the North Sea, at approximately 60 km from the coast in Pleistocene and Holocene sediments. The bathymetry reaches depths up to 38 m and the seafloor is largely devoid of bedforms (Arcadis, 2019).

During the Pleistocene epoch (2,58 Ma- 11,700 years ago) several glaciations followed by interglacial warming periods occurred, leading to local and regional changes in paleoenvironments across Northern Europe (Lamb. et al. 2018). The sedimentary record of TNW area registered three main glaciation episodes (Elsterian, Saalian and Weichselian) and associated interglacial cycles, which have shaped the area's geomorphology (Fig 1) (Ehlers 1990).

Wide depressions known as tunnel valleys and numerous channel systems were formed by oscillating movements of the ice sheets and dewatering processes which reshaped the landscape (Fig 1) (Huuse et Lykke-Andersen 2000). These features were later filled with heterogenous sediments, influenced by marine transgression and regression dynamics (Kirkham et al. 2024). Other features such as potholes, scour marks, kettles and subglacial lakes are also encountered. Since the last Weichselian glaciation (11,700 years ago), the sea level has continuously risen, leading to the present-day coastline.

Material and method

The dataset is composed of a 3D UHRS cube as well as ten CPT's over an area of 6.125 km². The data bin size is 50 cm, and the vertical resolution is 0.1 m. The frequency content ranges from 0 to 5000 Hz. To cope with the high resolution of UHRS, the data has been decimated by a factor of 2 to save time during calculations.

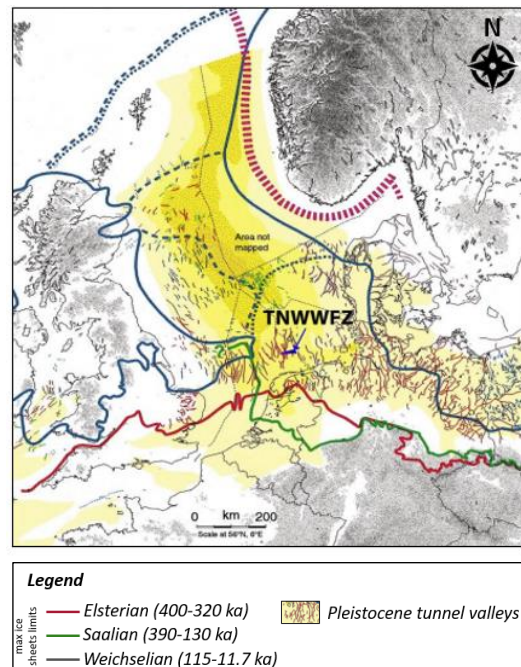


Figure 1: Maximum ice sheets limits during Pleistocene glaciation of the northwest Europe (source: RVO, 2019)

The integration and interpretation of the datasets mentioned above was carried out using PaleoScan™ software (Pauget et al. 2009). The first step consists in creating a discrete stratigraphic framework called the “Model-Grid” (Fig 2). This grid contains auto-tracked, stratigraphically sorted and editable seismic horizons within the volume (Peaks & Troughs for every 7 traces in this case study). In the second step, the interpolation of the Model-Grid allows the conversion of each horizon into continuous geological surfaces, resulting in the creation of a full 3D Relative Geological Time Model (RGT) (Fig 3). The third step consists in importing CPT logs of interest which are the normalised cone resistance and the friction ratio. The fourth and final step consists in propagating the CPT data within the RGT model to map static soil properties, calculated from the late Pleistocene epoch to the seabed.

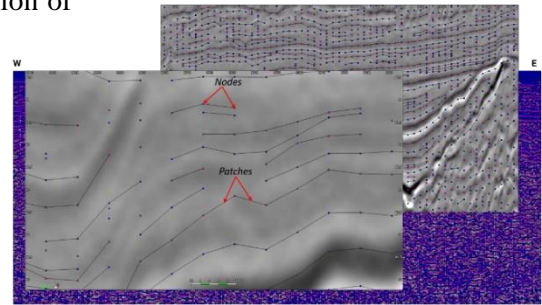


Figure 2: Zoom on the model-grid skeleton composed of nodes linked to patches.

Additionally, several attributes such as RMS, seismic amplitude and spectral decomposition (Fig 1) using frequencies of 390 Hz, 712 Hz and 1045Hz were calculated.

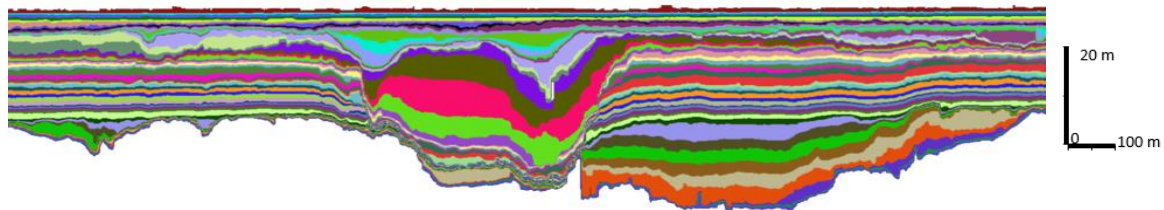


Figure 3: TNW RGT model

Results

In the western part of the survey, a deep and steep tunnel valley is trending from North to South. This erosive surface has been attributed to the Elsterian glaciation, occurring from 400 to 320 ka. In the shallowest part of the western section, two main channels also trending North-South, carved by glacial melting water and glaciotectionics during the Last Glacial Maximum (Fig 4). The infilling sediments show a different acoustic impedance signature on the RMS horizon stack and the spectral decomposition (Fig 5). This variation indicates differences in soil rheology between channels and the surrounding area.

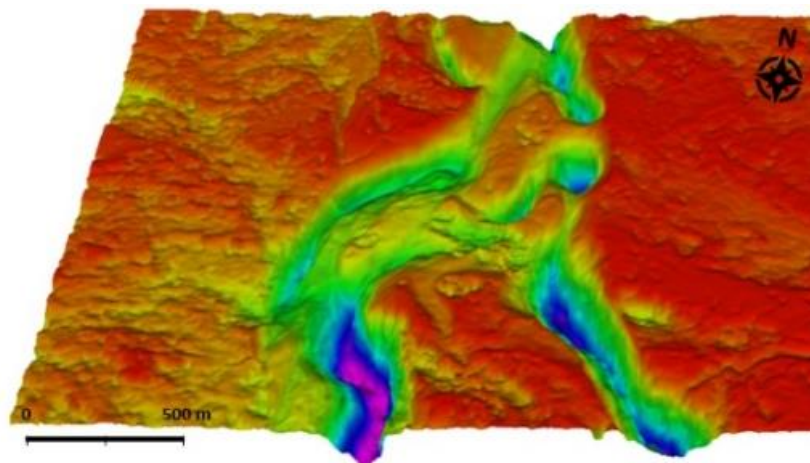


Figure 4: 3D view of the Weichselian channelised systems

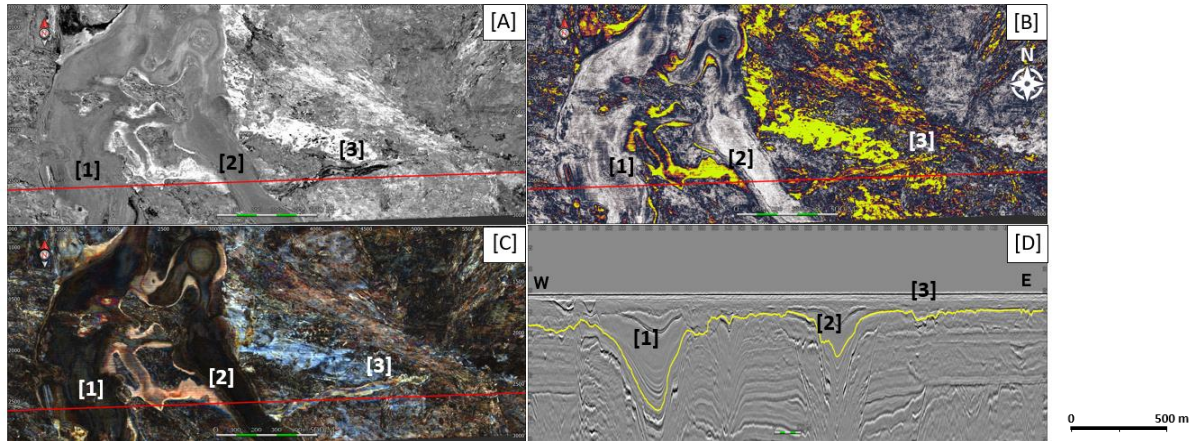


Figure 5 Seismic horizon stack [A] with RMS [B] and Spectral decomposition attribute [C] and profile 2587, showing Weichselian channel systems [1],[2] and [3].

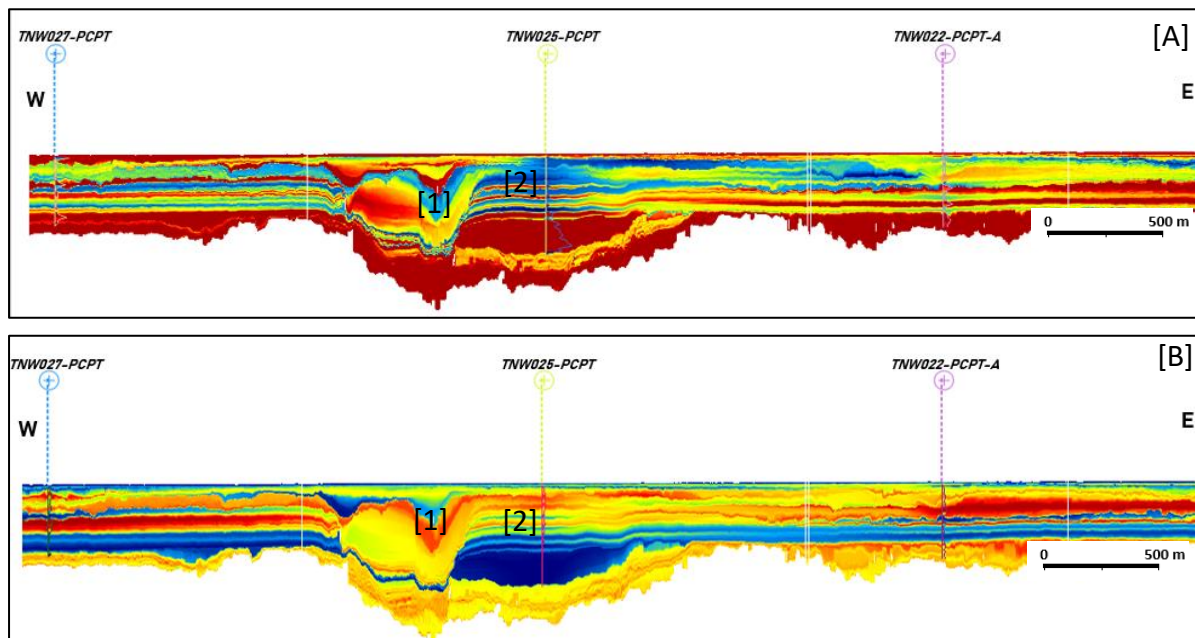


Figure 6 RGT and seismic based property models showing [A] Normalised friction ratio and [B] the normalised cone resistance parameter. Low Friction ratio (blue) indicates sandy materials or desiccated clays. High friction ratio (red) indicates clayey materials. Normalised cone resistance can be considered as an analogue of the shear strength. Blue values correspond to low penetration resistance; red corresponds to high penetration resistance.

All property models show significant lateral and vertical facies variations. This difference is even more striking within the channels.

Given the fact friction ratio (Fig 6 [A]) serves as a proxy for preliminary lithology interpretation, hypothesize about the nature of TNW sediments (Robertson 2009) arises : the bottom of the eastern channel (zone 1) is represented by a blue layer indicating sediments with a higher sandy fraction whereas the surrounding area (zone 2) shows thin variations between red (clay) and blue layers (sand). In the normalised cone resistance model (Fig 6 [B]), the blue colour indicates low resistance and soft soil, whereas red indicates coarse soil. The deeper part of both channels (zone 1) exhibits a red colour, suggesting a coarse layer while the shallower infill shows soft (blue) sediments. This infilling sequence could correspond to the usual fluvio-glacial sequence. Furthermore (zone 2) shifts from coarse to soft sediments but this is less pronounced.

Integrating Friction ratio and Normalised cone resistance property models allows us to hypothesize that the deeper infilling layer (zone 1) could be coarse sandy material with a soft clay layer above it. The sediment succession in zone 2 displays smoother transitions between soft clayey and coarse sandy layers. This alternation could correspond to regression-transgression cycles between the Saalian (290-130 ka) and Weichselian glaciations (115-11,7 ka).

These observations demonstrate high variability in soil properties within the channels compared to surrounding units.

Conclusions

Offshore wind farm development plays an important role in the energy transition market.

The detailed characterisation of the shallowest sedimental succession is crucial for mapping cable backfilling, wind turbine location and globally de-risking offshore wind farm installation.

The integration of 3D UHRS volumes and CPT's datasets is a powerful combination in geotechnical offshore engineering operations, enabling the efficient detection of small elements that could be considered as geohazards. Creating integrated property models displaying soil characteristics according to RGT models allows the interpreter to apprehend lateral and vertical facies variations with a 50 cm resolution. In conclusion, the use of semi-automated workflows in the Paleoscan™ software allowed for efficient handling of UHRS data and the integration of CPT logs to better understand the glacial geomorphology and the location of geo-engineering hazards.

Acknowledgements (Optional)

The author would like to thank the Netherlands Enterprise Agency (RVO) for providing datasets and associated reports written by Arcadis Nederland BV and Eliis for providing the Paleoscan™.

References

- Bellwald, Benjamin, Luke Griffiths, Ragnhild Hansen, J. Dujardin, Carl Forsberg, M. Gail, Carl Forsberg, et al. 2023. *Multi-disciplinary Characterization of Sedimentary Environments on Glaciated Margins: Implications for Engineering of Offshore Windfarm Sites*. <https://doi.org/10.3997/2214-4609.202320040>.
- Ehlers, Jürgen. 1990. « Reconstructing the dynamics of the North-west European Pleistocene ice sheets ». *Quaternary Science Reviews* 9 (1): 71-83. [https://doi.org/10.1016/0277-3791\(90\)90005-U](https://doi.org/10.1016/0277-3791(90)90005-U).
- Huuse, Mads, et Holger Lykke-Andersen. 2000. « Overdeepened Quaternary valleys in the eastern Danish North Sea: morphology and origin ». *Quaternary Science Reviews* 19 (12): 1233-53. [https://doi.org/10.1016/S0277-3791\(99\)00103-1](https://doi.org/10.1016/S0277-3791(99)00103-1).
- Kirkham, James D., Kelly A. Hogan, Robert D. Larter, Ed Self, Ken Games, Mads Huuse, Margaret A. Stewart, et al. 2024. « The infill of tunnel valleys in the central North Sea: Implications for sedimentary processes, geohazards, and ice-sheet dynamics ». *Marine Geology* 467 (janvier):107185. <https://doi.org/10.1016/j.margeo.2023.107185>.
- Lamb Rachel M., Harding Rachel, Huuse Mads, Stewart Margaret, et Brocklehurst Simon H. 2018. « The early Quaternary North Sea Basin ». *Journal of the Geological Society* 175 (2): 275-90. <https://doi.org/10.1144/jgs2017-057>.
- Pauget, F., Lacaze, S. et Valding, T. 2009. « A global approach to seismic interpretation base on cost function and minimization. », expanded abstract, 28 (1): 2592-96.
- Robertson, P. K. 2009. « Interpretation of cone penetration tests — a unified approach ». *Canadian Geotechnical Journal* 46 (11): 1337-55. <https://doi.org/10.1139/T09-065>.